This project sponsored by the Air Force Materiel Command

Photonic Band Gap Structures on Polymer Materials for Microstructure Waveguides and High-Speed Interconnects

Final Report

Contract No. F30602-94-C-0193

Period of Performance: 08/02/94 to 02/20/95

Presented to:

Rome Laboratory/IMPT
26 Electronic Parkway
Griffiss AFB, NY 13441-4514

Prepared by:

Physical Optics Corporation
Applied Technology Division
2545 West 237th Street, Suite B
Torrance, CA 90505

Principal Investigator:

Michael Wang, Ph.D.
(310) 530-1416

March 1995

REPORT DOCUMENTATION PAGE

Form Approved
OMB No. 0704-0188

1. AGENCY USE ONLY *(Leave blank)*	2. REPORT DATE	3. REPORT TYPE AND DATES COVERED
	03/02/95	Final 08/02/94 to 02/02/95

4. TITLE AND SUBTITLE
Photonic Band Gap Structures on Polymer Materials for Microstructure Waveguides and High-Speed Interconnects

5. FUNDING NUMBERS
F30602-94-C-0193

6. AUTHOR(S)
Michael Wang, Ph.D.

7. PERFORMING ORGANIZATION NAME(S) AND ADDRESS(ES)

Physical Optics Corporation
2545 West 237th Street, Suite B
Torrance, California 90505

8. PERFORMING ORGANIZATION REPORT NUMBER
3284

9. SPONSORING / MONITORING AGENCY NAME(S) AND ADDRESS(ES)

Rome Laboratory
26 Electronic Parkway
Griffiss AFB, NY 13441-4514

10. SPONSORING / MONITORING AGENCY REPORT NUMBER

11. SUPPLEMENTARY NOTES

Accesion For
NTIS CRA&I
DTIC TAB
Unannounced
Justification
By
Distribution /
Availability Codes
Dist | Avail and / or Special
A-1

12a. DISTRIBUTION / AVAILABILITY STATEMENT

Unlimited

12b. DISTRIBUTION CODE

13. ABSTRACT *(Maximum 200 words)*

Physical Optics Corporation (POC) proposed a new concept of creating photonic band gaps on optical waveguides for the realization of low loss bands. These low loss bands are particularly useful for the realization of high density optical interconnection networks for multi-chip modules and other single-board high-speed functional circuits. In the Phase I program, POC focused on the structures that can be used to construct waveguide photonic band gap structures, namely 2-D and 1-D PBG structures. The understanding of these structures and a theoretical study of their contributions to optical beam confinement have been achieved. We further examined their operational properties, including polarization dependence and material index differential requirements. Beam confinement conditions for a large range of off-axis beam angles have been identified between two 1-D PBG structures, which is the basis for the construction of low loss waveguide bands. This strong beam confinement for large angle off-axis beams is not achievable in conventional optical waveguides based on total internal reflection. The applications of the waveguide PBG structures include high density optical interconnect buses, waveguide filters, micro-ring tunable filters and lasers, switches, and integrated wavelength division mulipliexers.

14. SUBJECT TERMS
Photonic Band Gap, Integrated Optics, Waveguide, Optical Interconnects

15. NUMBER OF PAGES
40

16. PRICE CODE

17. SECURITY CLASSIFICATION OF REPORT	18. SECURITY CLASSIFICATION OF THIS PAGE	19. SECURITY CLASSIFICATION OF ABSTRACT	20. LIMITATION OF ABSTRACT
Unclassified	Unclassified	Unclassified	SAR

TABLE OF CONTENTS

LIST OF FIGURES

LIST OF FIGURES (Cont)

1.0 INTRODUCTION

Many new discoveries in Physics have resulted from the study of wave propagation in periodic structures. Analogous to the behavior of electrons in semiconductor lattices with band gaps which prohibit certain electron energies, the behavior of photons in three-dimensional dielectric structures has led to the recent discovery of Photonic Band Gaps (PBGs) [1-3] that prevent certain photon energies or wavelengths from propagating. Radiation with photon energies above the level of the gaps would transmit through the material. In-gap radiation from outside the material would be reflected, while in-gap radiation inside the material would be trapped. Filtering, noise suppression, and the suppression of spontaneous emissions in highly efficient lasers are some potential applications that could result from the development of the PBG structures and materials.

Currently, most of the research work being performed on PBGs is theoretical [4-14]. PBGs have been experimentally demonstrated only at microwave frequencies in high-index dielectric materials which are drilled into face-centered cubic (FCC) structures [1,15], and in 3-D arranged periodic dielectric rods [16]. To obtain a PBG at optical wavelengths, a "lattice" spacing of submicron periodicity is required. With such a small periodicity, the creation of a 3-D PBG structure is extremely difficult. The race is currently underway to demonstrate an optical PBG using reactive ion-beam etching on GaAs. However, no success has been reported at optical wavelengths. Experimental efforts to demonstrate a waveguide PBG at optical wavelengths would be much easier, but have also not yet been reported.

To date, the applications of photonic band gap structures have not been fully explored. Some applications have been mentioned above. None of them has been realized at optical wavelengths, due to the difficulty in creating 3-D PBG structures with submicron periodicity. In this program, Physical Optics Corporation (POC) investigated planar optical interconnects using waveguide optical buses, a new application of the PBG structure for the reduction of channel waveguide bending loss.

In Phase I, POC proposed to study a waveguide photonic band gap structure on polymer for the realization of ultra-low-loss optical waveguide bends for the optical interconnection of high-speed electronics for wafer-scale integration and multi-chip module (MCM) applications. The significance of the proposed concept for interconnects is as follows. As shown in Figure 1-1, optical waveguides are used to interconnect high-speed electronic chips on the board level. The sharp optical waveguide path bends required for some of these optical buses may cause significant bending losses due to escaping radiation. Conventional waveguides confine optical waves in the high index channel region through the total internal reflection (TIR) principle. In sharply bent structures, the TIR condition may not be satisfied, and significant bending losses may result. Typically, the bending loss becomes significant when the radius of the bend is smaller than 5 mm (or 5000 μm). This is considered large when compared to channel widths of less than 5 – 10 μm, typical in practical optical bus applications. The losses depend on the curvature of the waveguide bends, and may range from several dB to several tens of dBs. This may degrade the performance of the interconnect buses and make the interconnect schemes unacceptable for some high-density packaged systems. Figure 1-2 shows the proposed concept of utilizing PBG structures to reduce the bending losses in sharply bent optical waveguides. Radiation escaping from the waveguide is prevented by the PBG structure, which causes the radiation to be reflected back and confined in the waveguide.

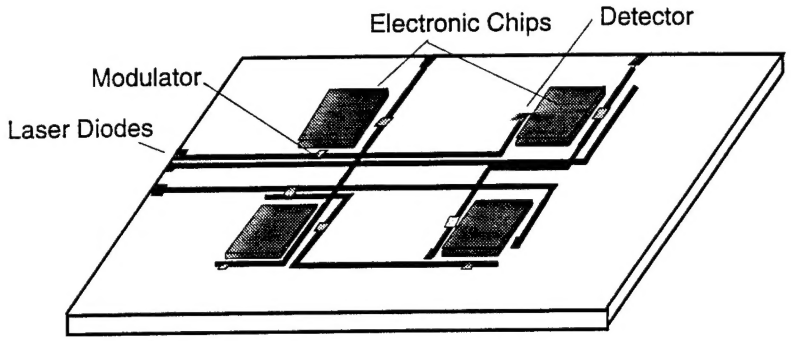

Figure 1-1
Optical interconnects based on low loss waveguide buses.

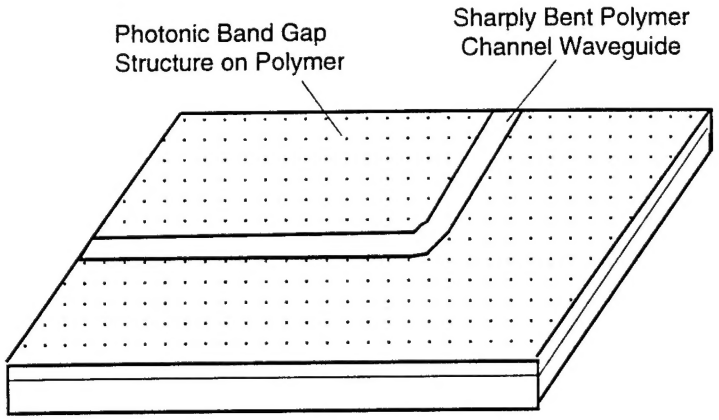

Figure 1-2
Low loss sharply bent optical waveguides using photonic band gap structures.

The Phase I research, as proposed, was essentially a feasibility study of a photonic band gap structure for the reduction of channel waveguide bending loss. Different from conventional optical waveguides based on total internal reflection for beam confinement, the proposed PBG structure confines optical beams by reflecting and establishing standing waves (or modes) between two PBG structures. The accomplishment of the Phase I work can be summarized as follows.

1. We studied the principle of the photonic band gap structures. We gained a general understanding of 1-D, 2-D, and 3-D photonic band gap structures. Both 1-D and 2-D photonic band gap structures were found useful for the construction PBG-based channel waveguides.

2. We identify that there is no existing theory that can be used to analyze the confinement of light beams between two PBG structures. The establishment of such theory is important for the design of waveguide photonic band gap structures on any waveguide, including polymer waveguides.

3. The formulation for confining light beams between two 1-D PBG structures with an arbitrary spacing in between the structures has been performed in Phase I. The results are promising, and show that the realization of a PBG-

based waveguide is possible. The required PBG feature size is achievable using conventional fabrication techniques.

4. We studied 2-D PBG structures for the confinement of light beams. This study showed that larger step index differences (about 0.4) are required to establish the desired band gaps.

5. The use of etching for the realization of polymer waveguide PBG structures is possible. Some high precision reactive ion-beam etching processes with submicron accuracy can be performed by QP-Semiconductor, Inc. However, the present cost is high (about $15K), due to the new engineering process, which requires a non-recurring engineering fee. Lower costs are possible for future commercial devices with established fabrication processes. Because of the higher cost, the experimental study for low bending loss waveguide PBGs must be postponed to Phase II.

In short, the Phase I study of the confinement of light by two photonic band gap structures has been fruitful, resulting in a potentially publishable technical contribution. Since it is an enabling technology, we believe that it will have significant effects on the demonstration of PBGs at optical wavelengths, the construction of PBG-based waveguides for waveguide lasers, the realization of low bending loss waveguides for wafer and board level optical bus interconnects, the development of miniaturized ring waveguide lasers and ring crossbar switches, and the development of integrated optical delay lines for phased-array applications.

2.0 THEORY FOR PHOTONIC BAND GAP STRUCTURE

2.1 Historical Review of Photonic Band Gap Structures

The electron energy band structure in a semiconductor is well understood: an electron's momentum is modulated by a lattice of ions, resulting in a forbidden electronic energy band gap. Valence band electrons spend most of their time near atoms with low potential energies, while conduction band electrons are found between atoms. A photon in a regular 3-D lattice of cavities in a dielectric material of high refractive index will experience similar momentum modulation. The photon can be concentrated in the high-index portion of the material ("atoms") or in the low index region between "atoms". The resulting forbidden photonic energy band is similar to that of electrons in a semiconductor.

The reason that this analogy can be established is due to the fact that the wave equations in periodic dielectric media are similar to the Schrodinger's equations in semiconductors. It is based on the Bloch expansion theorem, which both electrons and photons obey in their corresponding lattice structures. An electromagnetic wave propagating through a periodic medium will generate multiple traveling waves in directions such that the resulting pattern of interference fringes matches the periodicity of the periodic structure. Any wavevector can be turned into any other by adding or subtracting an integral multiple of grating vectors, **K**, of the periodic structure. The Bloch waves of an extended periodic medium consist of stable superpositions of many such waves. The simplest case is the Bragg condition, when the fringe pattern matches the periodicity of the medium and Bragg diffraction occurs, preventing power flow across the structure.

To better understand the behavior of the photonic band structure, consider a one-dimensional periodic medium. This is similar to a multilayer dielectric coating. Figure 2-1 shows a periodic dielectric medium with evenly spaced high and low refractive indices.

Stop-bands open up around the Bragg conditions in k-space. In the Bragg condition, the power flow through the structure is prevented. Away from the Bragg condition, the transmitted beam experiences either in-phase or out-of-phase energy distribution in the periodic medium. For in-phase distribution, as shown in the lower part of Figure 2-1, most of the energy is distributed in the high index medium. A higher refractive index implies a shorter effective wavelength. Thus, in order to satisfy the condition that the fringe pattern match the periodicity, the vacuum optical wavelength must be longer or the photon energy must be smaller. This is why low energy photons appear mostly in the high index portion of the periodic structure. Photons in this case are in the "valence" band. For out-of-phase distribution, as shown in the upper part of Figure 2-1, most of the energy is distributed in the low index medium. To satisfy the same periodicity, a lower vacuum optical wavelength is required. Photons in this case have higher energy, and are situated mostly in the low-index portion of the structure. Photons in this case are in the "conduction" band. The energy between these two cases (i.e., in the photonic band gap) is reflected due to Bragg diffraction. The bandwidth of the Bragg diffraction is the gap width. As the step index difference of the periodic structure increases, there are more Fourier components which can cause significant reflection; the photonic band gap widens. When the periodic structure is a sinusoidal index distribution, there is no band gap, since there are no other Fourier components. As long as there are Fourier components, there is a band gap, in principle, no matter how small the index difference is.

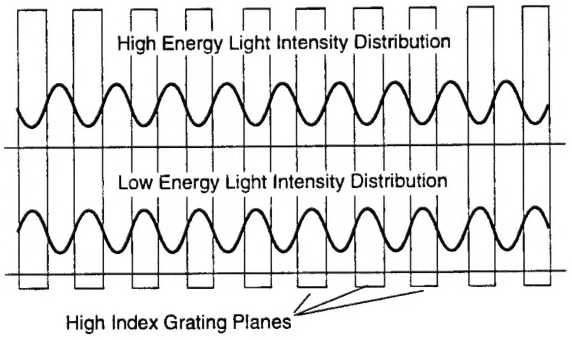

Figure 2-1
Schematic of a one-dimensional PBG structure showing optical energy distribution [2].

When this principle is applied to 2-D and 3-D space, it creates 2-D and 3-D photonic band gaps, respectively. The discovery of the photonic band gap structure occurred through the pioneering efforts of Eli Yablonovitch of Bellcore, U.S. (now at the University of California, Los Angeles), and of Sajeev John of the University of Toronto, Canada. Yablonovitch published the initial report in 1987. Since then, extensive research activities have been reported by a number of authors and research institutions, including Jonathan Dowling and Charles Bowden of the Weapons Sciences Directorate of the U.S. Army Missile Command in Alabama; Robert Meade et al. of the Department of Physics at MIT; T. K. Gaylord et al. of Georgia Institute of Technology; K. M. Leung of the Department of Physics at the Polytechnic University in New York; K. M. Ho of Iowa State University; M. Fleischhauer et al. at the University of New Mexico; A. A. Maradudin of the Department of Physics at the University of California, Irvine; and D. R. Smith and S. Schultz of the Department of Physics at the University of California, San Diego. Other theoretical work has also been reported (see references).

A 3-D PBG structure is formed when a dielectric of high refractive index is riddled with a regular 3-D lattice of cavities. Experimentally, 3-D PBG structures have been created by drilling micro cavities with FCC structures into high index dielectrics [15] or by stacking dielectric rods [16] (see Figure 2-2). Due to the large periodicity, these 3-D PBG structures have demonstrated band gaps at microwave frequencies only. Theoretical work using vector wave equations matches well with experimental measurements.

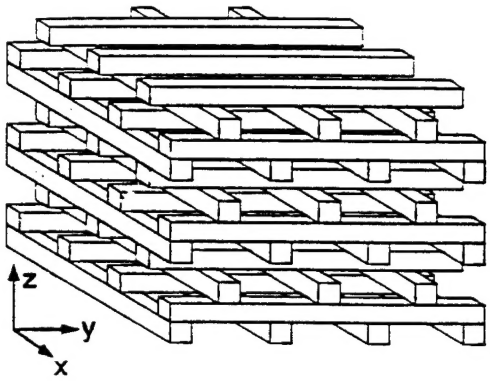

Figure 2-2
3-D photonic band gap structures.

A 2-D PBG structure can be created by arranging dielectric rods in a 2-D periodic format. The theoretical work for this was pioneered by A. A. Maradudin of the Department of Physics at the University of California, Irvine, R. Meade of the Department of Physics at MIT, and D. R. Smith and S. Schultz of the Department of Physics at the University of California, San Diego. Again, the theoretical and experimental results match well at microwave frequencies, but no experimental results have been demonstrated in the optical regime.

A 1-D PBG structure can be created through multilayer periodic dielectric coatings. This theory is described in the book, "Optical Waves in Crystals," by Yariv and Yeh. Recently, in 1993, a paper entitled "Photonic band structures and defects in one and two dimensions" was published by D. R. Smith et al. There is excellent agreement between theory and experimentation. Again, however, the major experimental efforts were in the microwave regime. No report has been identified describing optical confinement between two PBG structures.

2.2 Photonic Band Gap Structures on Waveguides

When a wave propagates and diffracts in a two-dimensional space, the existence of a periodic photonic "lattice" structure perpendicular to the 2-D plane has no effect on the momentum modulation of the propagating wave. A 2-D photonic "lattice" structure is sufficient to describe the behavior of the wave propagation. In reality, the fabrication of the 2-D photonic band-gap structure is simpler than that of the 3-D case. The periodic cavity holes in the 3-D case become 2-D periodic cavity tunnels (or rods), as shown in Figure 2-3. The tunnels can be drilled or etched. The rods can be placed. There is no complicated multilayer hole alignment in this case. Any incident wave in the 2-D case, in

practice, has no infinitely wide energy distribution. 2-D theory can be effectively used, as long as the depths of the tunnels exceed the width of the wave energy distribution in the direction perpendicular to the 2-D plane.

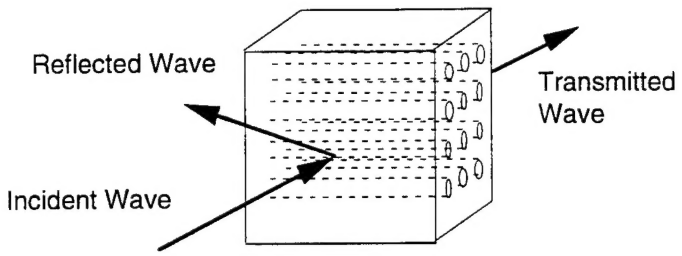

Figure 2-3
2-D wave propagation and 2-D PBG structures.

An optical planar waveguide is an example of 2-D wave propagation. The propagating wave is confined in the waveguide medium by total internal reflection. The propagating wave vector is modified using an effective waveguide refractive index, rather than a bulk material index. In the waveguide plane, the wave propagates like a 2-D wave. Perpendicular to the plane, the wave's energy distribution is controlled by the waveguide index distribution and the mode number of the wave. Waveguide index distribution can be achieved through multilayer coating of different materials, ion exchange, or other index perturbation techniques. When 2-D holes of a regular photonic "lattice" structure are generated in the plane, a 2-D photonic band structure is formed in the waveguide (see Figure 2-4). The depth of these cylindrical holes perpendicular to the waveguide should be comparable to or longer than the waveguide mode energy distribution depth. Otherwise, some degree of boundary scattering may occur in the direction perpendicular to the waveguide plane. Fortunately, most single mode waveguides or waveguides with just a few modes confine optical energies within depths ranging from submicron to a few microns. Drilling or etching cylindrical cavities of such depth should be much easier than fabricating 3-D PBG structures.

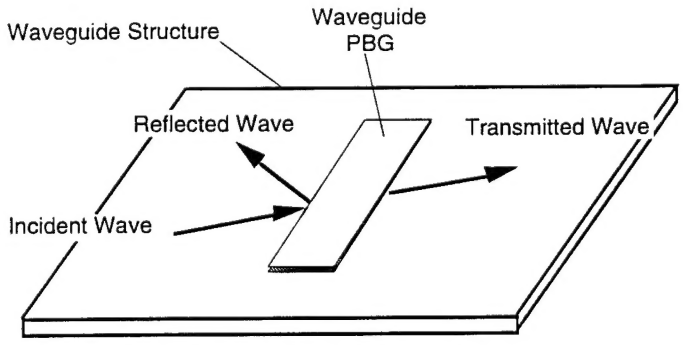

Figure 2-4
2-D waveguide mode propagation in the waveguide PBG structure.

The waveguide PBG structure shown above has a 2-D geometry. Depending on the application, the waveguide PBG can also use a 1-D geometry, as shown in Figure 2-5. Here, periodically etched slots in the waveguide plane can also reflect guided beams when

the energy is within the band gap, and transmit guided beams when the energy is above or below the band gap. This structure functions like a waveguide Bragg mirror, except that the frequency or wavelength bandwidths for the beams to be reflected are much wider. The 1-D waveguide PBG structure is simpler than a 2-D waveguide PBG for the above reflection applications. When the waveguide PBG structure is used to create y-branching junctions, as shown in Figure 2-6, a 2-D waveguide PBG structure becomes necessary.

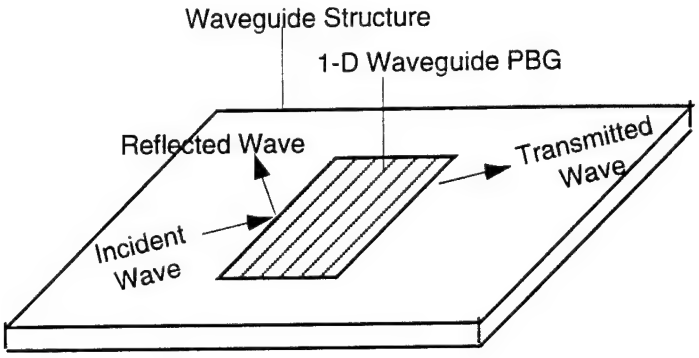

Figure 2-5
Guided beam reflection and transmission from an 1-D waveguide PBG structure.

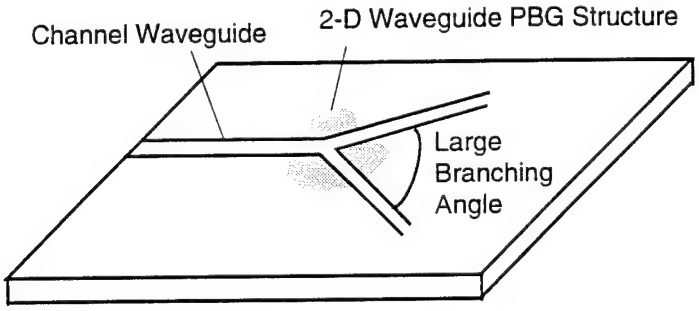

Figure 2-6
2-D Waveguide PBG for Y-branching junction application. Large branching angle is possible in this case.

In general, photon energies within the photonic band gap are reflected, while those outside the photonic band gap are transmitted. For the waveguide PBG structure, this is still true. When the optical frequency falls outside the gap of the waveguide PBG structure, the planar waveguide beam will be transmitted through the PBG structure, as was shown in Figures 2-4 and 2-5. When the optical frequency falls inside the gap of the waveguide PBG structure, the planar guided beam will be reflected by the PBG structure. A trade-off exists between the angular and frequency bandwidths for high reflectivity. Perfect reflection will be obtained for a single-frequency wave over a finite angular bandwidth, and for a perfectly collimated beam over a finite range of frequencies. To achieve complete reflectivity over a large spread of solid angles and over as wide a range of frequencies as possible, the index modulation of the periodic structure must be large [1,2]. In general, a planar guided wave will be either transmitted or reflected, depending on the PBG structure and the frequency of the light. A waveguide PBG can thus be used to generate a wide range waveguide wavelength filters.

2.3 The Concept of Constructing a Channel Waveguide in a PBG Structure

Since the guided beam is reflected by the PBG structure when the frequency of the light is within the photonic band gap, a channel waveguide can be formed in the waveguide PBG structure. Vertical confinement of the channel waveguide can be achieved by total internal reflection using conventional waveguide-index profiling in the depth direction. The channel waveguide's lateral confinement can be achieved by multiple reflections from the two waveguide PBG structures shown in Figure 2-7. Figure 2-7(a) shows a channel waveguide formed by 2-D waveguide PBG structures, while Figure 2-7(b) shows a channel waveguide formed by 1-D waveguide PBG structures. Since the reflection from the PBG structure is highly efficient for designated wavelengths, and material absorption is prohibited in the PBG, these channel waveguides should demonstrate ultra-low loss characteristics. The channel waveguide mode is determined by the creation of standing waves between the two PBG structures and vertical waveguide confinement. Both 2-D and 1-D waveguide PBGs can be used for the channel formation purposes. The simplest way is to use a 1-D waveguide PBG structure for channel waveguide formation. This 1-D structure has a lower requirement on periodic index differences as compared to the 2-D structure. This issue will be discussed in the following theoretical sections. This can make 1-D PBG formation easier. For example, a 1-D waveguide PBG can be created through optical exposure for periodic index differences, rather than by etching, which is somewhat more complicated. Furthermore, the 1-D PBG structure has low polarization dependence, making it ideal for a variety of device applications. In contrast, the 2-D PBG is highly polarization dependent. The 2-D PBG structure, however, can find applications in polarization control.

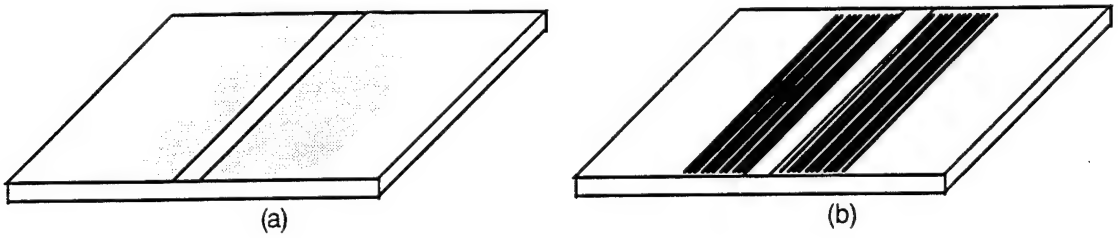

Figure 2-7
Formation of channel waveguide using waveguide PBG structures. (a) Using 2-D PBG structure; and (b) Using 1-D PBG structure.

In the following sections, we will discuss the properties and differences of 2-D and 1-D PBG structures. The requirement for a large index difference and the large polarization dependence of a 2-D PBG structure will be shown. The focus of our formulations will thus be given to 1-D photonic band gap structure for the waveguide formation. The 1-D waveguide PBG is more practical than the 2-D one for the proposed application.

2.4 Basic Properties of 2-D Photonic Band Gap Structure

In this section, we will discuss the properties the 2-D PBG structure, which will show the essential physics for band gap formation, and requirement for index differences and polarization dependent effects.

The geometry which will be considered in this section is that of an array of dielectric cylinders, periodic in two dimensions, and infinite in length in the third dimension. The radius of a cylinder is r, and the distance between the cylinders (the lattice constant) is d. We assume here that the propagation takes place in the plane of the lattice. There are two types of modes which exist in this case; namely, the electric field polarized along the cylinder axes (TM modes), and the magnetic field polarized along the cylinder axes (TE modes). A triangular lattice structure is analyzed. The theory for this structure has been reported earlier [11] without considering the beam confinement properties of the proposed study.

The essential properties of a photonic lattice can be summarized in a plot of its band structure. The band structure is a graphical depiction of the frequency vs. lattice momentum (k) dispersion relation for a specific periodic structure. The minimum region of k-space for the dispersion relation is the well known First Brillouin Zone (BZ) in solid state physics. In order to obtain the band structure for a PBG lattice, the appropriate wave equation must be solved. For the 2-D PBG structure shown in Figure 2-8, Maxwell's equations reduce to the following scalar equations:

$$-\nabla^2 E_z(\bar{x}) = \varepsilon(\bar{x})\frac{\omega^2}{c^2}E_2(\bar{x}) \tag{2-1}$$

for TM modes, and

$$\nabla x\left(\frac{1}{\varepsilon(\bar{x})}\nabla x\left(H_z(\bar{x})\bar{z}\right)\right) = \frac{\omega^2}{c^2}H_z(\bar{x}) \tag{2-2}$$

for TE modes. The permeability is assumed to be unity. The periodicity of the medium has the translation invariance relationship for the dielectric function

$$\varepsilon\left(\bar{x}+\bar{R}\right) = \varepsilon(\bar{x}) \tag{2-3}$$

where R is a primitive translation vector. Thus, to satisfy Bloch's theorem, we have

$$f(x+R) = \varepsilon^{ik\cdot R}f(x) \tag{2-4}$$

where f(x) refers either to E_z or H_z, and **k** is known as the Bloch vector.

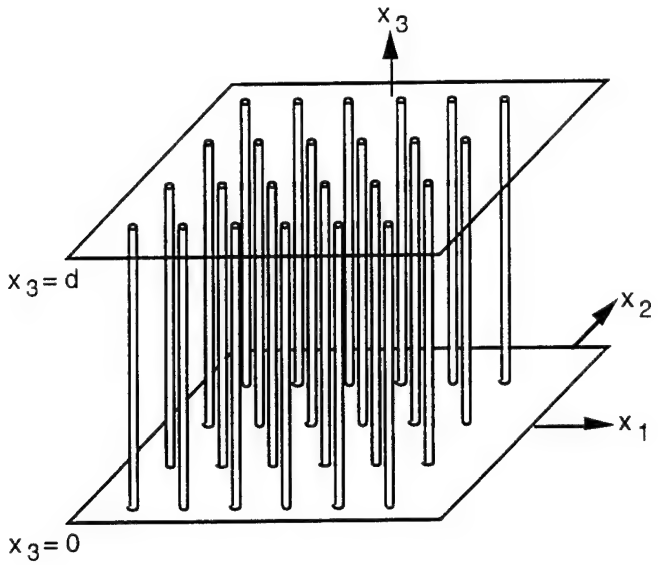

Figure 2-8
Schematic of a 2-D PBG structure.

The wave equations above are subject to the boundary condition, and can be solved over a single unit cell of the repeated lattice. For each Bloch vector **k**, there exists an infinite set of eigenfrequencies which can be indexed as $\omega_{k,i}$, where i is known as the band index. As a function of k, the solutions $\omega_{k,i}$ form a continuous surface, periodic in k space, which can be identified as the band i. The plot of all of these surfaces vs. k constitutes the band structure. While the pass band frequently overlaps, there may be regions of frequency for which some directions of k do not intersect any of the $\omega_{k,i}$ bands. When this condition occurs, there is said to be a photonic band gap in that direction. If there exists a range of frequencies which do not intersect with a pass band for any value of **k** (i.e., if there is no overlap between adjacent pass bands), then the set of frequencies is termed an absolute photonic band gap.

The solutions for these band frequencies can be performed through a solution of eigenvalue problems [11]. For TE modes, the eigenvalue matrix equation is

$$\sum_{G'}(k+G)\cdot(k+G')\hat{k}(G-G')A(k\mid G')=\frac{\omega^2}{c^2}A(k\mid G) \tag{2-5}$$

where G is a vector of the lattice reciprocal, and $\hat{k}$ and A satisfy the Fourier transform equations

$$\frac{1}{\varepsilon(x)}=\sum_{G}\hat{k}(G)e^{iG\cdot\bar{x}} \tag{2-6a}$$

$$H_z(x\mid\omega)=\sum_{G}A(k\mid G)e^{i(k+G)\cdot\bar{x}} \tag{2-6b}$$

Similarly, for TM modes, the eigenvalue equation for frequency is given by

$$\sum_{G'} |k+G|\hat{k}(G-G')|k+G'|C(k\,|\,G') = \frac{\omega^2}{c^2} C(k\,|\,G) \tag{2-7}$$

where C is given by

$$C(k\,|\,G) = |k+G|B(k\,|\,G) \tag{2-8}$$

with

$$E_2(x\,|\,\omega) = \sum_G B(k\,|\,G) e^{i(k+G)\cdot\bar{x}} \tag{2-9}$$

Figure 2-9 shows a calculated band structure for the TE mode under $n_a = 1$ and $n_b = 1.6$ with filling factor r/d = 0.34. Clearly, there is an absolute photonic band gap (shaded area) which prevents light beams of frequencies within this band from propagating. We note that the frequency is scaled according to the periodicity d. Similar calculations for TM modes give the band structure shown in Figure 2-10. There is no observable band gap for this polarization. Thus, the band gap is polarization-dependent.

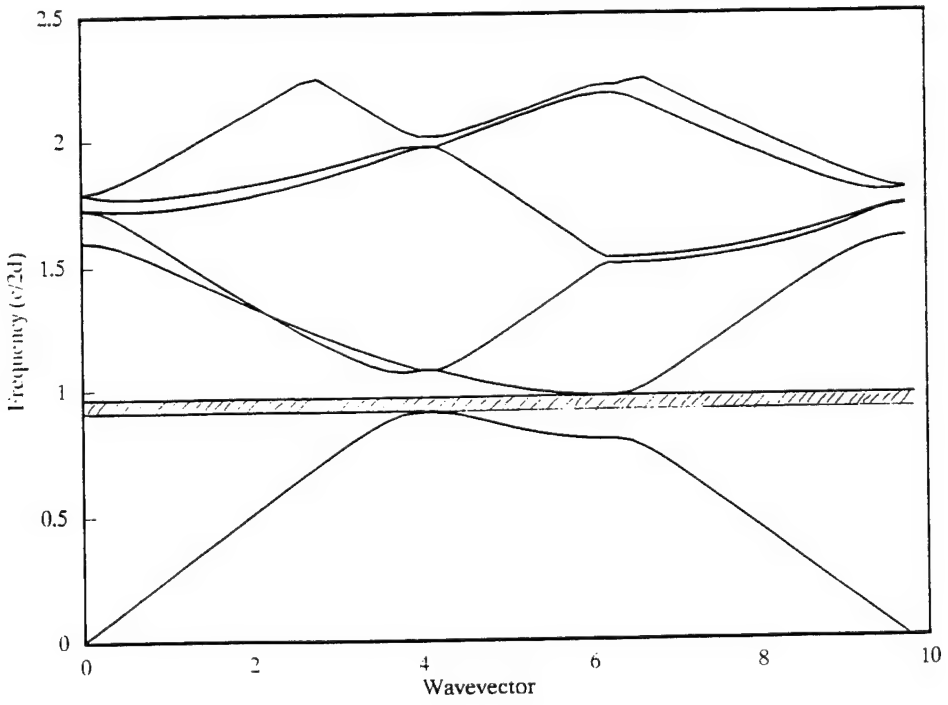

Figure 2-9
Calculated photonic band gap for TE modes. For the calculation, $n_a = 1$, $n_b = 1.6$, and r/d = 0.34. The absolute band gap exists at f = 0.94 (c/2d).

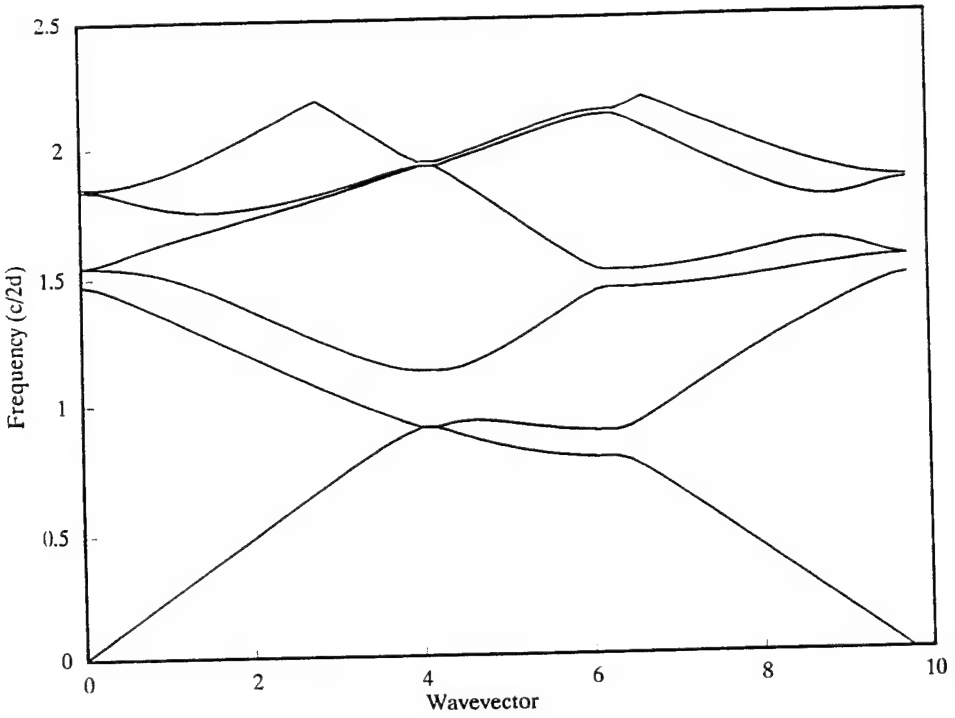

Figure 2-10
Calculated photonic band structure for TM modes. For the calculation, $n_a = 1$, $n_b = 1.6$, and r/d = 0.34. There is no observable absolute band gap.

Furthermore, a calculation of the results shown in Figure 2-11, performed by A. A. Maradudin [11], shows a dielectric cut-off for photonic band gaps. For TE modes, the lowest dielectric ε_b for the band gap to exist is about 2. Thus, the minimum background material index is about 1.414 with drilled cylindrical holes of index 1.0. For TM modes, the minimum ε_b is 6, and the minimum background index is 2.45.

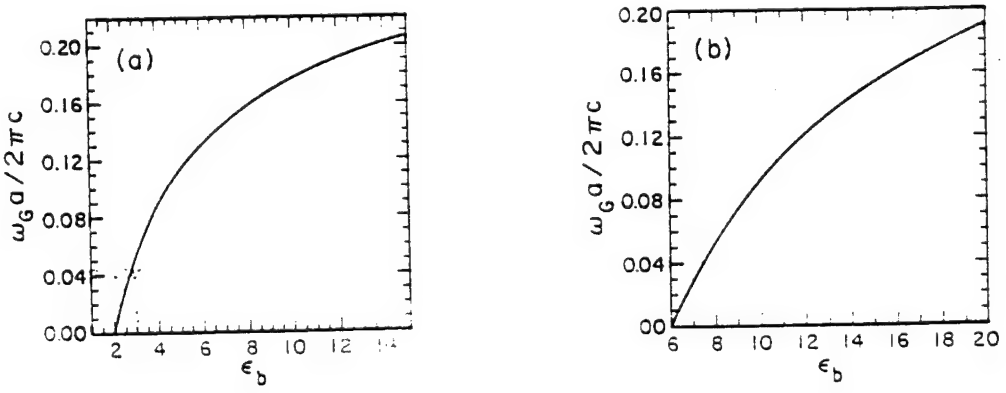

(a) (b)

Figure 2-11
The width of the absolute band gap as a function of contrast at the optimum filling factor for that contrast. (a) TE modes, s = 1; (b) TM modes, s = 1.

On a polymer waveguide, creating photonic band gap structures by drilling or etching periodic cylindrical holes is possible. The PBG is only applied to TE modes, since most polymer materials have indices of less than 1.8.

2.5 Advantages and Disadvantages of 2-D Waveguide PBG

The above calculation for the 2-D PBG structure provides us with the following guidelines (including advantages and disadvantages) for creating waveguide PBG structures:

1. When the material index is less than 1.41 it is not possible to create 2-D PBG structures.

2. It is only possible to create absolute band gap structures for TE modes when the material index is less than 2.45.

3. Absolute band gaps exist for both TE and TM polarized modes when the material indices are larger than 2.45. However, the overlapping of TE and TM band gaps largely depend on the structure used. The 2-D photonic band gaps are highly polarization-dependent.

4. At this moment, there is no published work addressing the confinement of light by two finite 2-D PBG structures, as shown in Figure 2-7(a), where the middle region is the channel waveguide. This problem is complicated.

In the Phase I program, due to time and budget constraints, we did not further address this 2-D PBG based waveguide problem. Instead, a simpler 1-D solution has been identified below.

2.6 Theory of 1-D Photonic Band Gap Structure

One-dimensional photonic band gap structures can be analyzed using a simple scalar wave equation for TE modes

$$\frac{\partial^2 E(x,y,t)}{\partial x^2} = \frac{n(x)^2}{c^2} \frac{\partial^2 E(x,y,t)}{\partial t^2} \tag{2-10}$$

where $n(x) = n_1$ or n_2 is the refractive index of the periodic material. The coordinates for this analysis are given in Figure 2-12. Solutions to Eq.(2-10) in any local region are combinations of left and right traveling waves. These solutions must also be continuous at the interfaces between different media, as must be their derivatives, set by the boundary conditions. Assuming the time dependence $E(x,y,t) = E(x,y)e^{-i\omega t}$, Eq.(2-10) becomes

$$\frac{\partial^2 E(x,y)}{\partial x^2} = \frac{n^2\omega^2}{c^2} E(x,y) \tag{2-11}$$

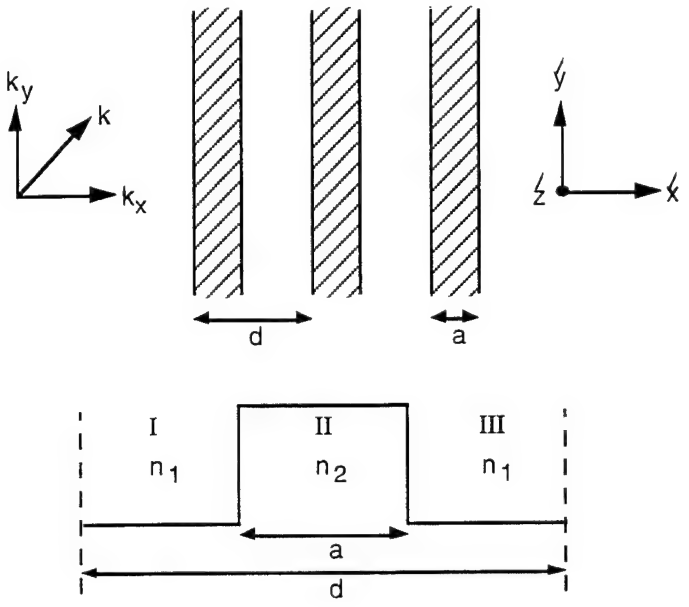

Figure 2-12
Model of 1-D PBG Structure

In each region, Eq.(2-11) yields the usual plane wave solutions with arbitrary coefficients, which we write as

$$E_I(x,y) = Ae^{ik_x x}e^{ik_y y} + Be^{-ik_x x}e^{ik_y y}$$

Region I:

$$E_{II}(x,y) = fe^{iq_x x}e^{iq_y y} + ge^{-iq_x x}e^{iq_y y} \qquad (2\text{-}12)$$

Region II:

$$E_{III}(x,y) = fe^{ik_x x}e^{ik_y y} + De^{-ik_x x}e^{ik_y y}$$

Region III:

where k_x is the horizontal component of **k**, k_y is the vertical component of **k**, and $k = n_1\omega/c$. Similarly, q_x and q_y are horizontal and vertical components of **q**, respectively, with $q = n_2\omega/c$. Applying the boundary condition

$$E_I\left(-\frac{q}{2},y\right) = E_{II}\left(-\frac{a}{2},y\right)$$

$$\frac{\partial}{\partial x}E_I\left(-\frac{a}{2},y\right) = \frac{\partial}{\partial x}E_{II}\left(-\frac{a}{2},y\right) \qquad (2\text{-}13)$$

$$E_{II}\left(\frac{a}{2},y\right) = E_{III}\left(\frac{a}{2},y\right)$$

$$\frac{\partial}{\partial x}E_{II}\left(\frac{a}{2},y\right)=\frac{\partial}{\partial x}E_{III}\left(\frac{a}{2},y\right)$$

and the continuity of phase $k_y = q_y$ and the translation invariance equation

$$E(x+d,y)=e^{i\mu d}E(x,y) \tag{2-14}$$

we obtain the dispersion relation of the PBG structure for the TE mode case

$$\cos(\mu d)=\cos[k_x(d-a)]\cos(q_x a)-\frac{1}{2}\left(\frac{k_x}{q_x}+\frac{q_x}{k_x}\right)\sin[k_x(d-a)]\sin(q_x a) \tag{2-15}$$

where μ is the momentum of the PBG structure and

$$k_x=\sqrt{\frac{n_1^2\omega^2}{c^2}-k_y^2}$$
$$q_x=\sqrt{\frac{n_2^2\omega^2}{c^2}-k_y^2} \tag{2-16}$$

Based on these equations, we have calculated the band structure (photon frequency band vs. k_y) of the periodic PBG structure. For the calculation, we use $n_1 = 1$, $n_2 = 1.4$, and filling factor $a/d = 0.5$. The calculated result is shown in Figure 2-13. It can be clearly seen that by adjusting the period of the structure the band gap can exist at any wavelength of interest. The existence of an absolute band gap for large k_y implies that it is possible to confine light beams between two 1-D PBG structures with large non-normal incident angles. This is important, since large incident angles are typical for conventional waveguide structures.

There is also no cut-off on the choice of material index. Figure 2-14 shows a band structure for $n_2 = 1.52$, very close to $n_1 = 1.5$, with $a/d = 0.5$. In other words, absolute band gaps exist for any finite index contrast. This is different from the 2-D PBG structure.

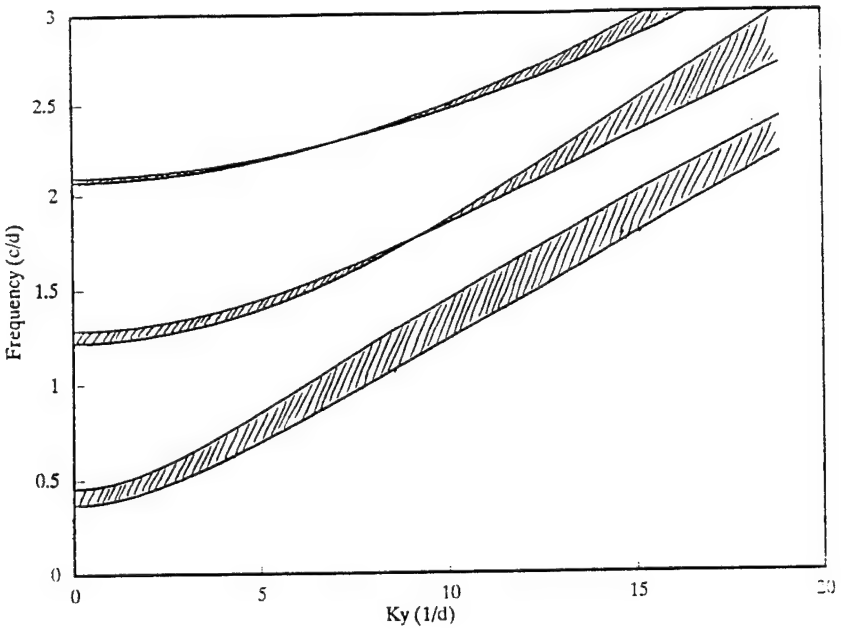

Figure 2-13
Calculated band structure as a function of k_y. The existence of absolute band gaps at large k_y implies that it is possible to confine light beams between two PBG structures for the formation of channel waveguides. For the calculation, we assume the value of n_1 = 1.0, n_2 = 1.4, and filling factor a/d = 0.5

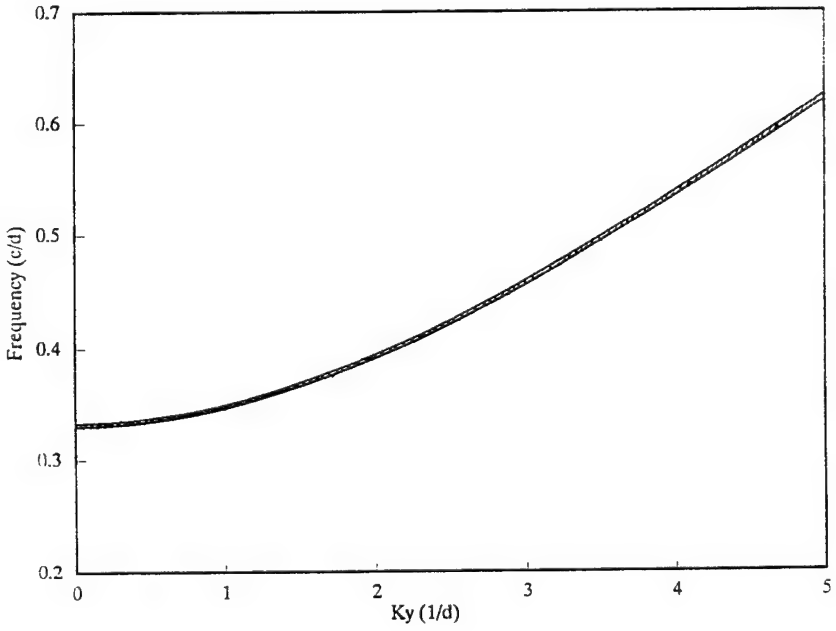

Figure 2-14
Calculated band structure under small index contrast showing that there is practically no cut off for band gaps in the 1-D geometry. For the calculation, we use n_1= 1.5, and n_2 = 1.52 and a/d = 0.5.

To determine the polarization dependence, we need to determine the band structure for TM modes. The wave equation for TM modes is

$$-\nabla^2\bar{H} = \frac{\omega^2}{c^2}\varepsilon_r\bar{H} \tag{2-17}$$

This equation is similar to the TE case, and thus the wave solution is also similar. The only difference between the TE and TM cases is the boundary condition

$$\begin{aligned} H_I\left(-\frac{a}{2},y\right) &= H_{II}\left(-\frac{a}{2},y\right) \\ \frac{1}{n_1^2}\frac{\partial}{\partial x}H_I\left(-\frac{a}{2},y\right) &= \frac{1}{n_2^2}\frac{\partial}{\partial x}H_{II}\left(-\frac{a}{2},y\right) \\ H_{II}\left(\frac{a}{2},y\right) &= H_{III}\left(\frac{a}{2},y\right) \\ \frac{1}{n_2^2}\frac{\partial}{\partial x}H_{II}\left(\frac{a}{2},y\right) &= \frac{1}{n_1^2}\frac{\partial}{\partial x}H_{III}\left(\frac{a}{2},y\right) \end{aligned} \tag{2-18}$$

The resulting dispersion relationship for TM modes is given by

$$\cos(\mu d) = \cos[k_x(d-a)]\cos(q_x a) - \frac{1}{2}\left(\frac{n_2^2}{n_1^2}\frac{k_x}{q_x} + \frac{n_1^2 q_x}{n_2^2 k_x}\right)\sin[k_x(d-a)]\sin(q_x a) \tag{2-19}$$

Figure 2-15 shows a calculated band structure for TM modes using the same geometrical configuration shown in Figure 2-12. Clearly, Figure 2-15 does not fully overlap with that of Figure 2-13. In some regions, there is overlap between TE and TM band gap regions. It is much easier to find common band gap regions between TE and TM for the 1-D case. Therefore, it is possible to construct non-polarization dependent PBG structures for particular incident conditions.

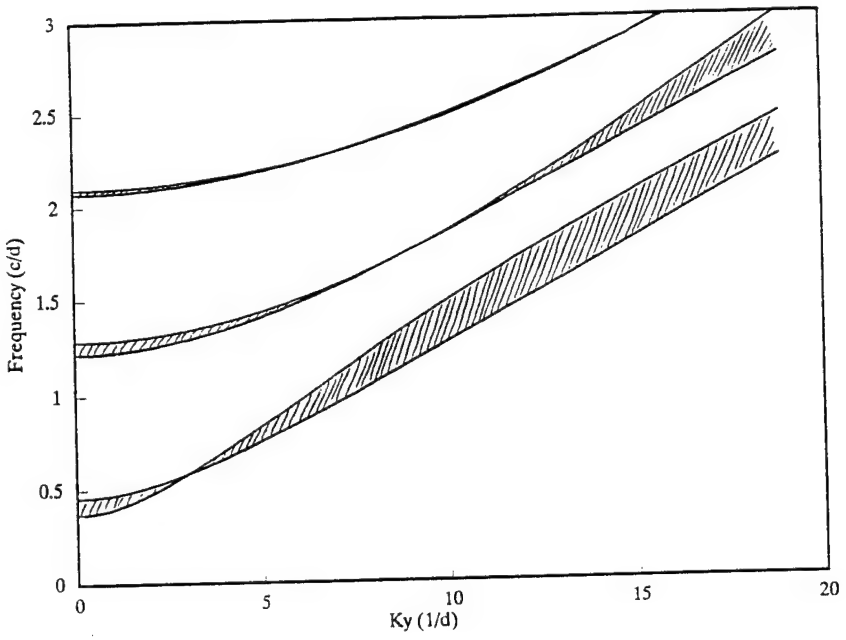

Figure 2-15
Calculated band gaps for a 1-D PBG structure under TM incident incidence. In many regions, the resulting band gaps overlap with the TE mode case of Figure 2-14.

2.7 Theory for Light Confinement Between Two 1-D PBG Structures

The theory presented in Section 2.6 applies only to an infinite 1-D PBG structure. When considering light confinement between two identical 1-D PBG structures with an arbitrary spacing, a modification is needed. Figure 2-16 shows an index distribution model for the analysis. Here, the middle region for the light confinement has a width of c, different from other dimensions like a and d. For this analysis, our coordinate is centered on the first n_2 region to the right of the confinement region.

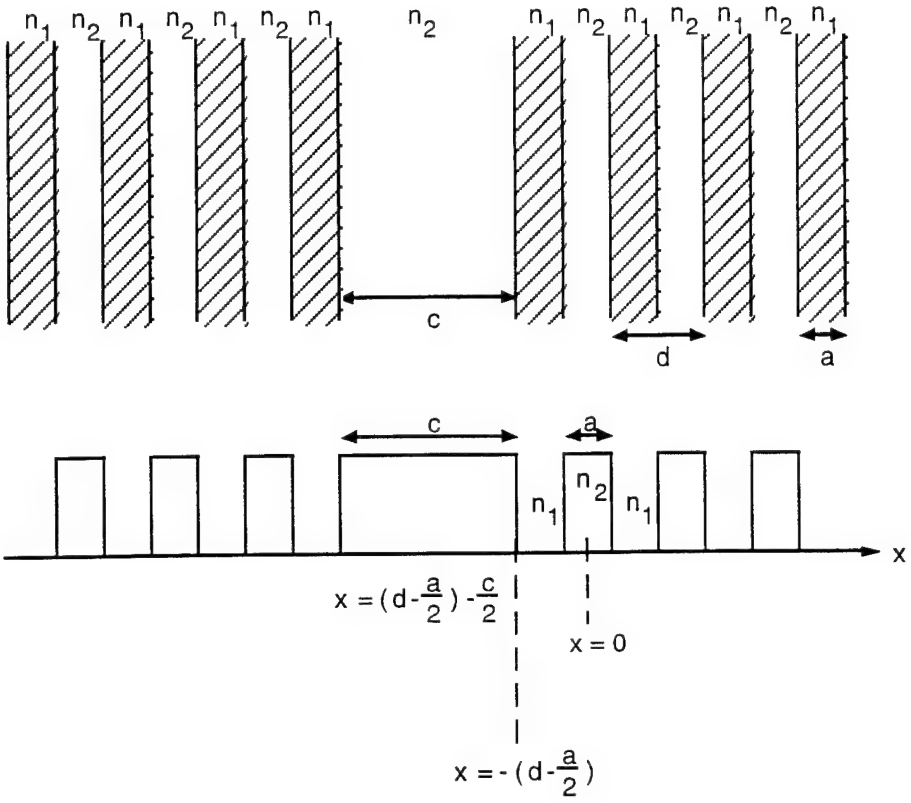

Figure 2-16
Coordinate system and index distribution for the light confinement analysis.

The TE field in the confinement region, by symmetry, must be

$$E_c(x) \propto \sin q\left[x + \left(d - \frac{a}{2}\right) + \frac{c}{2}\right] \quad \text{antisymmetric} \qquad (2\text{-}20)$$

$$\cos q\left[x + \left(d - \frac{a}{2}\right) + \frac{c}{2}\right] \quad \text{symmetric}$$

In the region next to the confinement region, the solution to the wave equation is

$$E_L(x) = Ae^{ik_x x} + Be^{ik_x x} = A\left(e^{ik_x x} + b^2 e^{ik_x x}\right) \quad b^2 = \frac{B}{A} \qquad (2\text{-}21)$$

Since we are looking for bound modes, we can have no energy transport; thus, A and B can only differ by a phase constant:

$$b^2 = e^{-i2\theta} \qquad (2\text{-}22)$$

Thus, we have

$$E_L(x) = Ab\left(e^{i(k_x x+\theta)} + e^{-i(k_x x+\theta)}\right) = 2Ab\ \cos(k_x x+\theta) = A'\cos(k_x x+\theta) \quad (2\text{-}23)$$

Matching the boundary conditions for symmetric modes, we have

$$\frac{q_x}{k_x}\tan\ q_x\frac{c}{2} = \frac{\tan\left[-k_x\left(d-\frac{a}{2}\right)\right]+\tan\theta}{1-\tan\left[-k_x\left(d-\frac{a}{2}\right)\right]\tan\theta} \quad (2\text{-}24)$$

$$\tan\theta = \frac{\frac{q_x}{k_x}\tan\left(q_x\frac{c}{2}\right)+\left(k_x\left(d-\frac{a}{2}\right)\right)}{1-\frac{q_x}{k_x}\tan\left(q_x\frac{c}{2}\right)\tan\left(k_x\left(d-\frac{a}{2}\right)\right)} \quad (2\text{-}25)$$

Applying the above results to the 1-D photonic band gap structure at the right hand side, repeating the derivation process in Section 2.6, we obtain the dispersion relation <u>for the TE mode case</u> as

$$\sin k_x(d-a)\cos q_x a + \frac{1}{2}\left(\frac{k_x}{q_x}+\frac{q_x}{k_x}\right)\cos k_x(d-a)\sin q_x a \quad (2\text{-}26)$$
$$= -\frac{1}{2}\left(\frac{q_x}{k_x}-\frac{k_x}{q_x}\right)\cos(k_x d-2\theta)\sin q_x a$$

Similar to Section 2.6, the dispersion equation can be modified for the <u>TM mode case</u> as

$$\sin k_x(d-a)\cos q_x a + \frac{1}{2}\left(\frac{n_2^2}{n_1^2}\frac{k_x}{q_x}+\frac{n_1^2}{n_2^2}\frac{q_x}{k_x}\right)\cos k_x(d-a)\sin q_x a \quad (2\text{-}27)$$
$$= -\frac{1}{2}\left(\frac{n_1^2}{n_2^2}\frac{q_x}{k_x}-\frac{n_2^2}{n_1^2}\frac{k_x}{q_x}\right)\cos(k_x d-2\theta)\sin q_x a$$

with

$$\tan\theta = \frac{\frac{n_1^2}{n_2^2}\frac{q_x}{k_x}\tan\left(q_x\frac{c}{2}\right)+\tan\left(k_x\left(d-\frac{a}{2}\right)\right)}{1-\frac{n_1^2}{n_2^2}\frac{q_x}{k_x}\tan\left(q_x\frac{c}{2}\right)\tan\left(k_x\left(d-\frac{a}{2}\right)\right)} \quad (2\text{-}28)$$

2.8 Calculation Results for the Light Confinement by Two 1-D PBG Structures

In order to establish light confinement between two 1-D PBG structures, the width c of the center region must be on the order of a wavelength or larger. The periodic regions in the PBG structure can, however, be smaller than the optical wavelength. The formulation in Section 2.7 provides a calculation freedom that enables us to arbitrarily choose the width of the confinement region. For a bent confinement structure, the major difference from a straight channel waveguide is that the off-axis incident angle is now larger. Because of this, the following calculations will consider the effect of incident angles and the confinement width c for light confinement between the two 1-D PBG structures.

Figure 2-17 shows excellent confinement of light beams between two 1-D PBG structures. For this calculation, the following parameters were used: $n_1 = 1$, $n_2 = 1.6$, $a/d = 0.5$, $c/d = 0.1$, and off-axis light angle is $\theta = 14°$. Most of the light beam is confined in a center region of width c. Very little optical power penetrates the PBG layer. The functionality of this confinement is similar to conventional optical waveguides. Increasing the width of c to c/d 0.2 does not result in any fundamental changes in the confinement properties (see Figure 2-18), except that the confined beam width increases accordingly. This is similar to conventional optical waveguides.

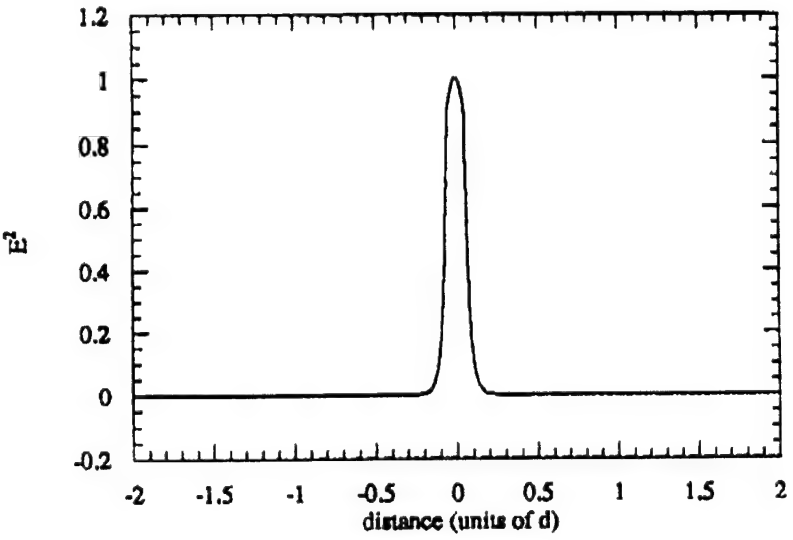

Figure 2-17
Confinement of light beam between two 1-D PBG structures. The ratio c/d is 0.1 and a/d of 0.5. The off-axis incident angle is 14°.

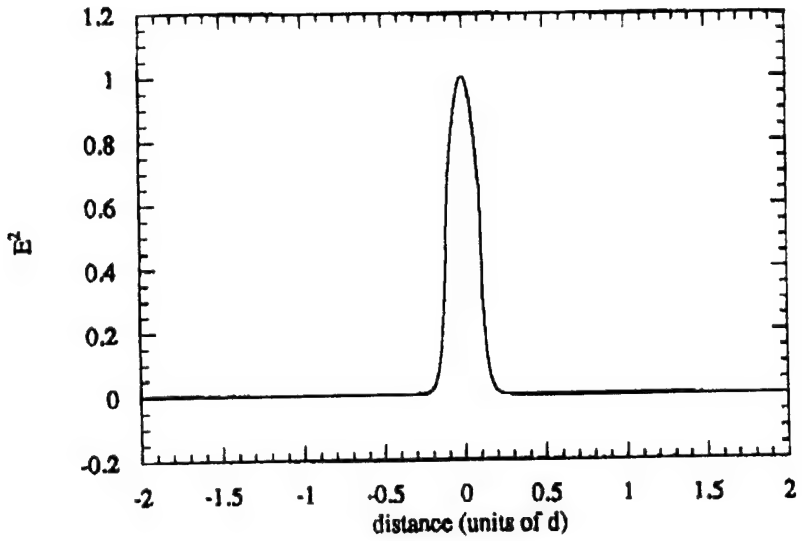

Figure 2-18
The calculated beam confinement for c/d = 0.2. All other parameters are the same as Figure 2-17.

Increasing the off-axis incident angle to 33° will result in the calculated beam confinement shown in Figure 2-19. Here again, the beam confinement is still excellent, with most of the beam energy located within the center region. This is particularly important, since it shows that increasing the angle of incidence will preserve the light confinement, and thus large bending of the structure will not result in any loss of optical power in the structure. This excellent beam confinement with such a large off-axis angle is a new feature introduced by the PBG structure compound. We can further increase the off-axis incident angle to 43.5° to introduce energy penetration to the PBG regions (see Figure 2-20). However, the energy penetration is limited, and the penetrated energy is not lost. In an extreme case, we have a 90° off-axis angle; the calculated results of this are shown in Figure 2-21, which shows that the light beam confinement is still reasonably good, with side lobes that represent the energy that penetrated into the PBG structure.

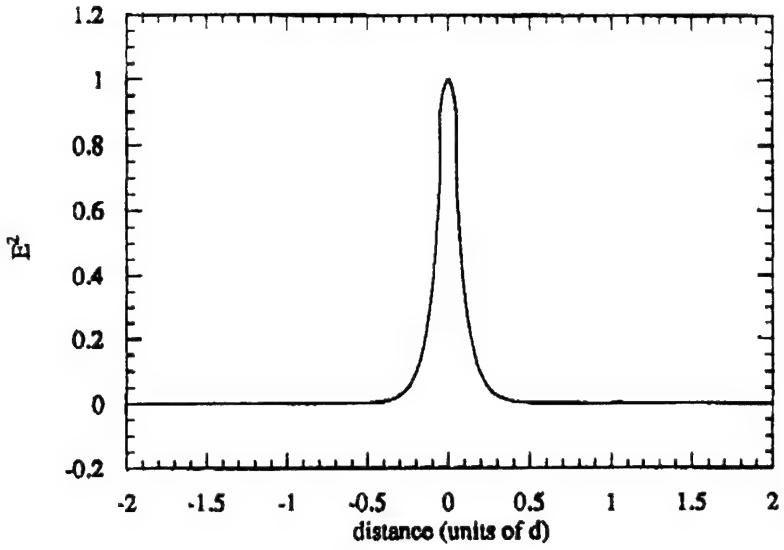

Figure 2-19
Increasing the off-axis incident angle to 33° results in no significant changes in beam confinement properties.

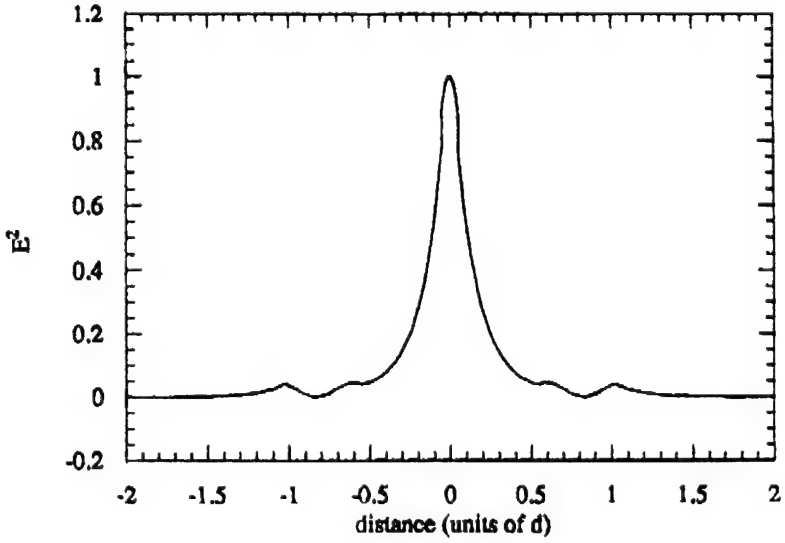

Figure 2-20
Increasing the off-axis angle to 43.5° results in slight beam penetration to the PBG regions with observable small side lobe features.

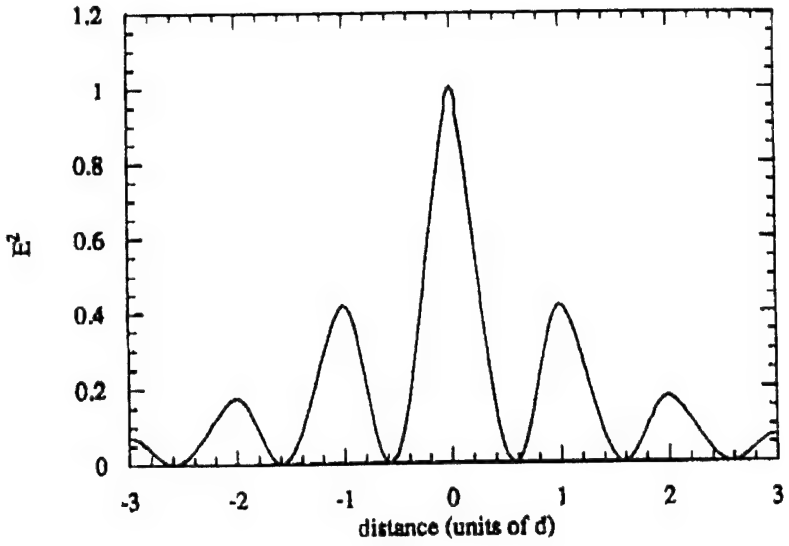

Figure 2-21
The calculated beam confinement under an extreme case, namely the off-axis angle of 90°. The beam confinement is still reasonably good. No optical power is lost by leakage.

2.9 Advantages and Disadvantages of 1-D PBG for Waveguide Formation

The above calculation for the confinement of light between two 1-D PBG structures provides us with the following guidelines (including advantages and disadvantages) for creating waveguide PBG structures:

1. There is no minimum requirement on the step index difference for the creation of a 1-D PBG structure.

2. In general, larger index differences result in larger photonic band gaps, and thus larger wavelength bandwidths and incident angle ranges for total PBG reflection.

3. Band gaps exist for both TE and TM modes. Polarization-dependent effects can be eliminated by selecting the proper index differences, wavelengths, and incident angles.

4. Confinement by two 1-D PBG structures is excellent. When the light beam is propagating normal to the structure, it creates standing waves with most of the energy located in the center confinement region. Away from this region, the wave energy rapidly decays in the PBG structures.

5. As the off-normal incident angle increases, more energy is confined in the center confinement region and less energy penetrates into the PBG structures.

6. At large off-normal incident angles, calculations indicate that no side lobes penetrate into the PBG regions. This case is similar to that of a

conventional waveguide, which confines light by total internal reflection within the confinement region.

7. When this structure is used to construct sharply bent waveguides, the bending portion may experience minimal energy penetration into the PBG structure. In this case, the total internal reflection condition may not be satisfied. However, the energy does not escape from the structure. Instead, it is reflected back by the 1-D PBG structure. High bending loss in conventional waveguides is thus prevented.

8. In a channel waveguide, the modes are generally hybrid; i.e., there are no purely TE or TM modes. The above formulation can still be applied when the polarization-insensitive region is identified.

Herein, we have shown that a simple 1-D PBG structure can be used to confine light beams by sandwiching two 1-D PBG structures. When this structure is used to provide lateral confinement of light in a waveguide plane, a new type of channel waveguide can be formed. This channel waveguide can eliminate bending loss, which is a serious problem for conventional channel waveguides based on total internal reflection for mode confinement. Detailed loss figures for the low loss bends will be measured in Phase II.

2.10 The Significance of Waveguide PBG Structure for Channel Bending Loss Reduction

It is well known that the bending of a dielectric channel waveguide will result in curvature-dependent radiation loss. This is due to partial radiation leakage from the guided mode to the unguided background. The loss can be significant when the bend is sharp. For example, a proton-exchanged channel waveguide on z-cut $LiNbO_3$ has a bending loss of about -4.5 dB for a 1 cm diameter bend. Low loss straight waveguides have been demonstrated on silica-on-silicon with losses of about -0.017 dB/cm. However, bending loss issues for these devices have not been solved. For bending radii of 5 mm or smaller, the loss is several dB to tens dB. Theoretical studies performed by Marcatili [18] and others [19,20] have substantiated the relationship between bending loss, channel width, channel index differential between core and surroundings, bending curvature, guided mode, and light wavelength. For example, as formulated by Marcatili [18], the loss per radian of a channel waveguide is

$$\alpha_c R = \frac{1}{2}\left(1-\frac{n_3^2}{n_1^2}\right)^{-\frac{1}{2}}\left(\frac{n_3 k_{x0} a}{n_1}\right)^2\left(\frac{A}{\pi a}\right)^3\left[1-\left(\frac{k_{x0}A}{\pi}\right)^2\right]^{\frac{1}{2}} \tag{2-34}$$

$$\cdot\frac{\Re\exp\left\{-\frac{\Re}{3}\left[1-\left(\frac{k_{xo}A}{\pi}\right)^2\left(1+\frac{2c'}{ak_{xo}}\right)^2\right]^{\frac{3}{2}}\right\}}{1-\left(1-\frac{n_3^4}{n_3^4}\right)\left(\frac{k_{xo}A}{\pi}\right)^2+2\frac{n_3^2 A}{n_1^2 a}\left[1-\left(\frac{k_{xo}A}{\pi}\right)^2\right]^{\frac{1}{2}}} \tag{2-35}$$

where

$$c' = \frac{1}{2k_{x0}a}\left(\frac{\pi a}{A}\right)^3 \frac{1}{\Re} \tag{2-36}$$

and

$$\Re = \frac{2\pi^3 R}{k_{z0}^2 A^3} = 2\frac{k_1^3}{k_{z0}^2}\left(1 - \frac{n_3^2}{n_1^2}\right)^{\frac{3}{2}} R \cdot \tag{2-37}$$

where k_{x0} and k_{z0} are channel waveguide propagating constants at corresponding coordinate axes when there is no bending. k_1 is the bulk propagating constant in the waveguide core. A is defined by

$$A = \frac{\lambda}{2\left(n_1^2 - n_3^2\right)^{\frac{1}{2}}} \cdot \tag{2-38}$$

The geometry for the channel waveguide is shown in Figure 2-22. A plot of TE-guided mode loss is shown in Figure 2-23. Note that, as c' decreases due to reduced curvature R, the loss per radian $\alpha_c R$ increases. The loss per radian also increases when the confined index differential $\Delta = (n_1 - n_3)/n_3$ decreases.

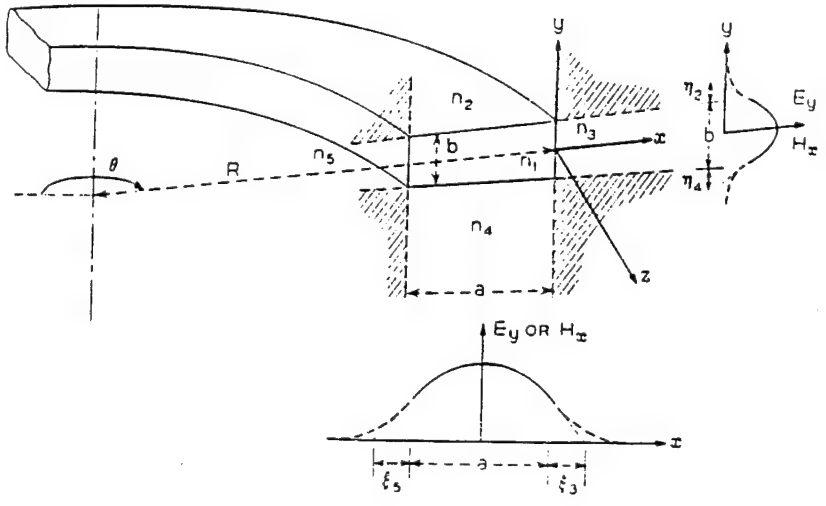

Figure 2-22
Parameters of conventional channel waveguides used in the formulation above [18].

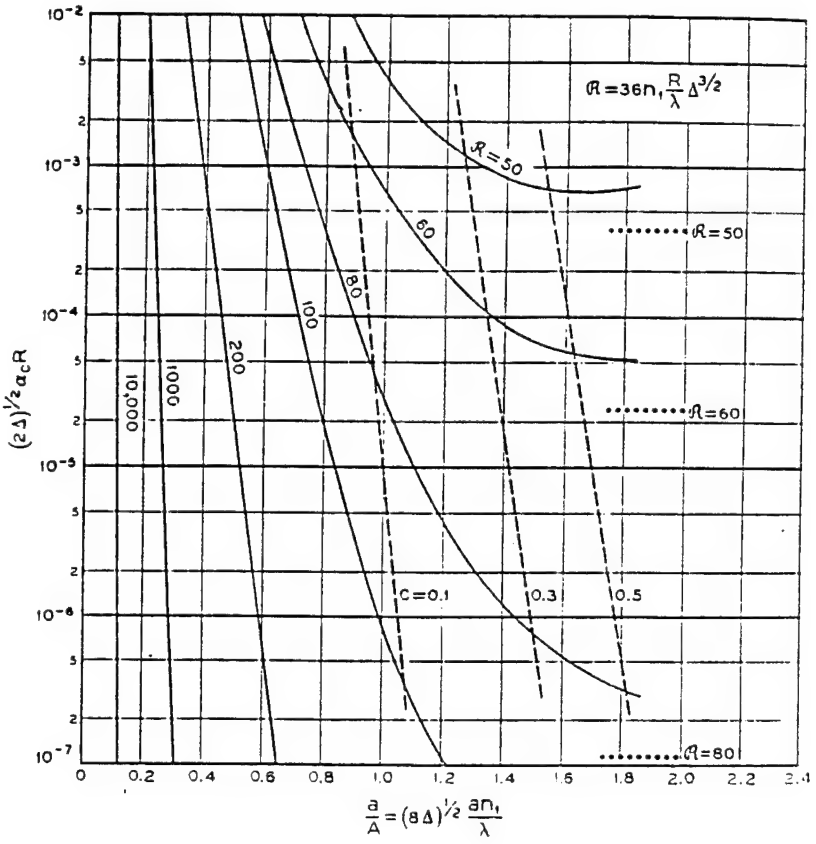

Figure 2-23
Calculated loss as a function of curvature and index difference for a fundamental TE mode [18].

The use of a waveguide PBG structure can totally eliminate the bending loss, since the PBG structure is highly reflective for light frequencies within the band gap. For a 1 mm banding radius or smaller, the incident angle is still quite large when we compare a channel of about 5 μm to a bending radius of 1000 μm. The angle changes from a straight channel to the bent channel should fall within the allowed angular region as specified by the angle dependent band gap structure.

The realization of an ultra low loss channel waveguide for both large and small bending curvatures will greatly enhance the flexibility of their use in board-level optical interconnection buses. It can also be used to construct integrated waveguide delay lines for phased-array applications, realize mini-ring waveguide filters for multiwavelength communications and crossbar switching, and develop mini-ring waveguide lasers. The applications are many. This will be addressed in Section 3.0.

2.11 Practical Considerations and Fabrication Guidelines

The ultimate goal of the Phase I study was to establish guidelines for constructing low bending loss channel waveguides. Based on the calculation results, we have determined

that it is possible to construct 2-D PBG structures for TE modes only with index differences larger than 0.42. This can be done on a waveguide by etching the waveguide material. For example, a polymer with index of 1.5 to 1.7 can be used to create planar waveguides. Etching the polymer can result in periodic index structures with index difference larger than 0.42, as was shown in Figure 2-7(a). The key issue on etching the structure is to make sure that the etched holes are deep enough (a few microns) so that the confined guided modes only see the cylindrical rod without experiencing the diffraction by its top and bottom boundaries. This can ensure that the 2-D theory in Section 2.5 can be applied. Due to the disadvantage of polarization dependence of the 2-D PBG for bending loss reduction applications, it is more favorable to use 1-D PBG structure, which is also simpler to fabricate.

Creating a 1-D PBG structure on a polymer is possible, since the polymer material can be etched with parallel slots, resulting a 1-D periodic index distribution. Since the 1-D PBG has no cut-off for the band gap, the refractive index difference on the periodic structure can be small. Thus, it is also possible to construct PBG structures using other means besides etching, such as the implantation of other materials and optical exposure on light sensitive materials. Again, we must make sure that the depth of the structure is a few microns so that the confined light beam will not interact with the upper and lower boundaries of the structure. When this condition is satisfied, the infinite 1-D model can be used.

The period of the 1-D PBG structure depends on the wavelength and the light incident angle. For light normally incident to the waveguide PBG structure, the calculated band gap in Figure 2-13 exists at a frequency of about 0.4 (c/d) or wavelength of 2.5 d. By choosing proper d, the PBG structure can be applied to visible or near infrared laser wavelengths. For example, we can pick the period d to be 0.58 μm. In this case, the band gap wavelength range is from 1.29 to 1.57 μm for a normally incident beam in a waveguide with an index of 1.6. When we consider an incident angle of around 75° to the structure (or Ry = .5d) , the band gap exists at a frequency of about 1.8 (c/d) or wavelength of 0.56 d. This time, the period can be larger. If we choose d to be 3 μm, the band gap wavelength range is from 1.5 to 1.71 μm. Under a fixed wavelength, the angular tolerance for total reflection by the PBG structure can be found in Figure 2-13. At a wavelength of 1.55 μm, near 75° incidence of 1.2 μm, and index difference of 0.6, we found that the angular tolerance is 2°

The construction of channel waveguides of low loss bends on polymer can be based on these results. The confinement calculation shows that we can choose the size of the confinement region to be about 5 μm.

When applications require deep channel waveguides (such as around 9 μm) to ensure mode profile matching with single mode fibers for communication applications, the etching slot must be deeper than 9 μm. In this case, it would be difficult to achieve uniform etching, since the depth of over 10 μm is much larger than the width of about 1 μm. In this case, we can consider using higher band gap frequencies; for example, the second or third band gap. This will greatly increase the period d under the same application wavelength. Increasing d makes such deep etching possible.

In practice, the etching can be performed by reactive ion beam etching or focused ion beam etching. Other non-etching techniques are also available for creating periodic structures with lower index differences.

3.0 POTENTIAL APPLICATIONS

This new concept and technique for constructing waveguide PBG structures on polymers can result in the realization of a variety of devices and technologies. It can be used to construct low-loss, sharply bent channel waveguides for board-level waveguide interconnects (see Figure 3-1) . Optical waveguide buses with sharp bends can significantly increase the packaging density of interconnect systems. Figure 3-1 shows a comparison of the effects of large bends and small bends on packaging density.

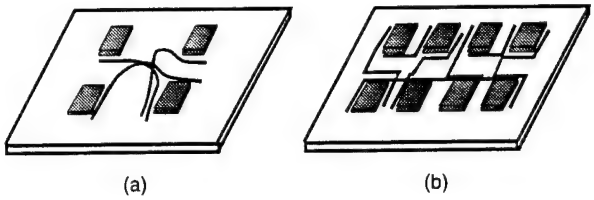

Figure 3-1
Comparison of packaging density using (a) conventional channel waveguides and (b) PBG channel waveguides. High density packaging can be achieved with low loss, sharply bent, PBG channel waveguides.

The waveguide PBG can also be used to construct waveguide notch filters, as shown in Figure 3-2. There can be planar waveguide notch filters and channel waveguide notch filters. The notch filter can be used for fiber communication applications to reflect a band of wavelengths, while permitting other wavelengths to be transmitted unimpeded.

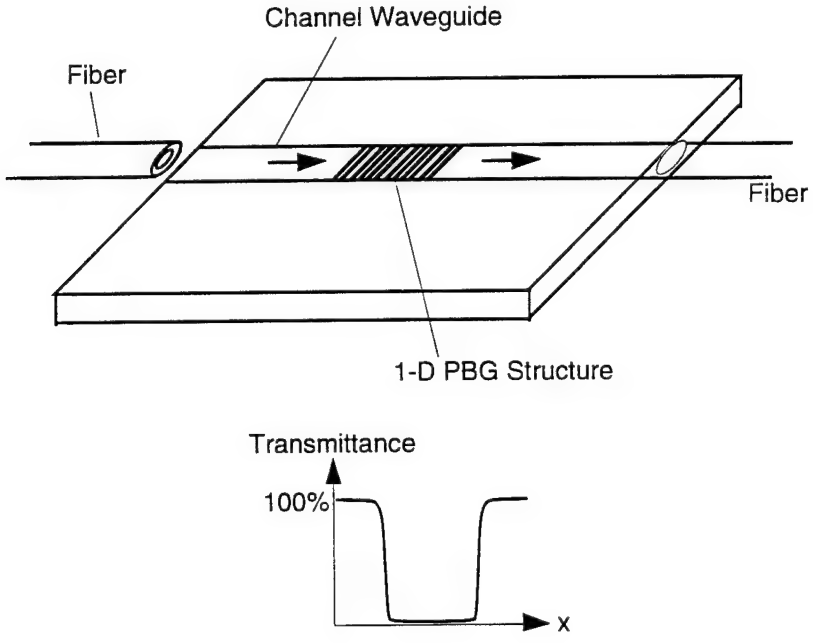

Figure 3-2
Waveguide notch filters.

The waveguide PBG structure can also be used to construct micro-ring devices with ring diameters of less than 2 mm. This would be the smallest ring achievable in practice. Applications for this can be found in electrooptic tunable wavelength filters, as shown in Figure 3-3.

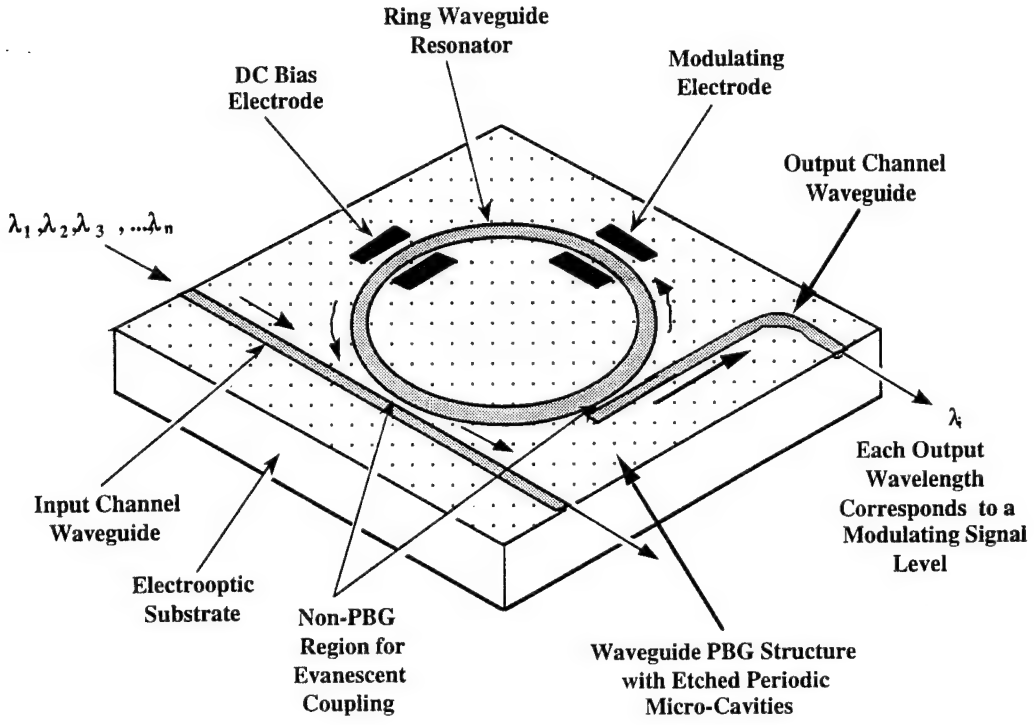

Figure 3-3
Waveguide PBG structure based micro-ring for wavelength filtering.

The same type of micro-ring can be used to construct multiwavelength electrooptic crossbar switches, as shown in Figure 3-4. This type of switch uses only 2N tunable ring switches to achieve N x N crossbar switching. This is a significant reduction of switch numbers as compared to conventional N^2 switches. The switching principle is follows. Any incoming signal wavelength, say λ_3, can be fed into the trunk waveguide after tuning the switching voltage on electrode #3 of the first switch group so that the ring resonant condition on ring #3 is satisfied. The signal propagation on λ_3 in the trunk waveguide can be selectively picked up by any of the switching elements of the second switch group by similarly tuning the ring resonance. Using this type of crossbar structure, any two-way non-blocking switching pattern can be realized with a minimum of 2N electrooptic switching elements. This includes one-to-many fanouts, many-to-one fan-ins, and many-to-many data communication patterns. This crossbar can also be used as a active wavelength division multiplexer and demultiplexer (see Figure 3-5).

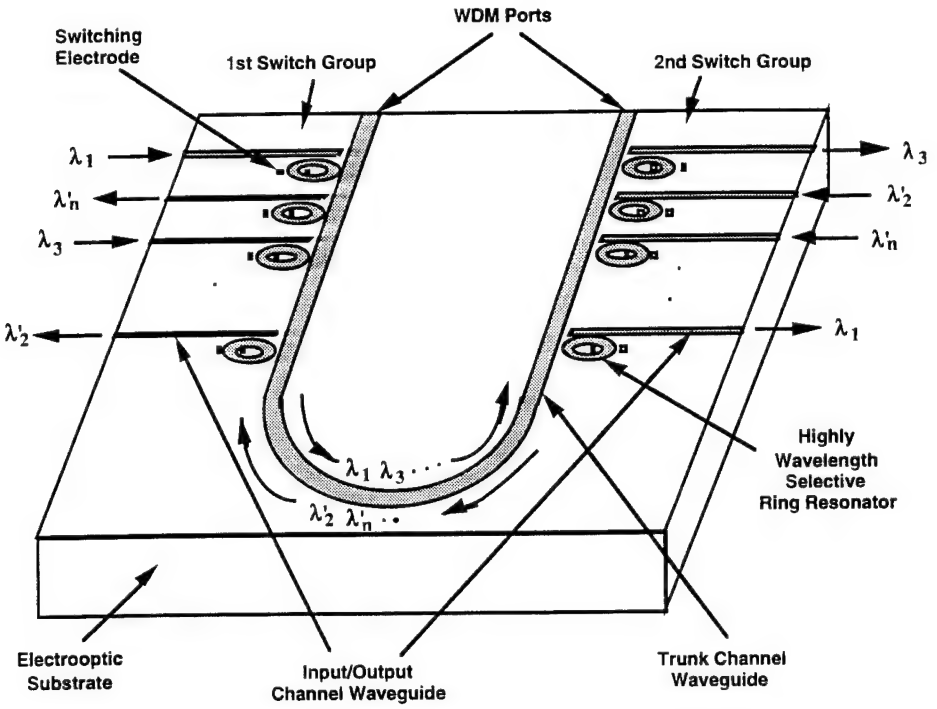

Figure 3-4
Use of PBG based micro-ring for multiwavelength N x N crossbar switching with only 2N switches.

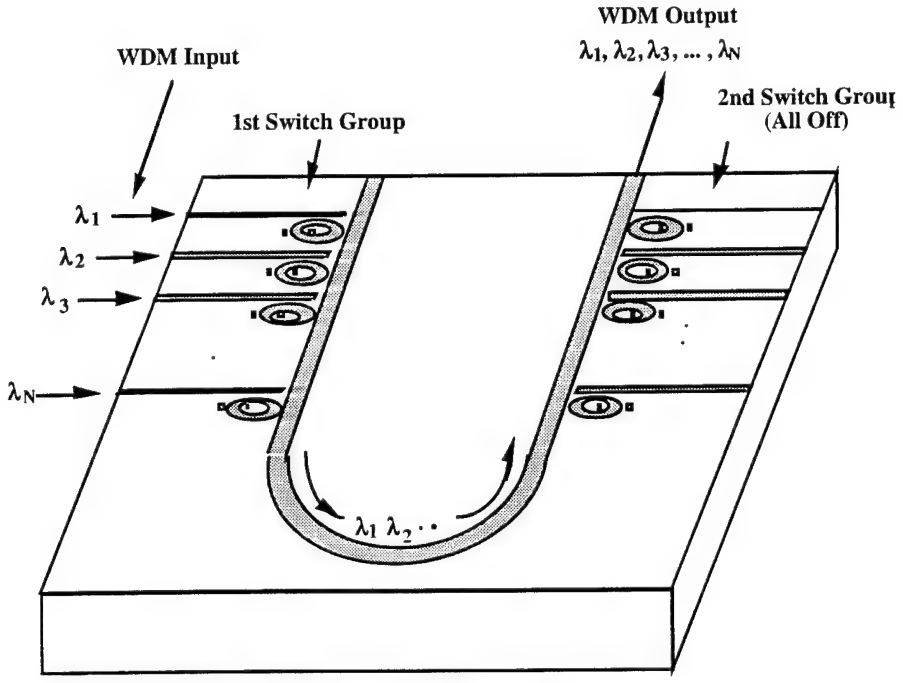

Figure 3-5
PBG based ring waveguide wavelength division multiplexer and demultiplexer.

The waveguide PBG structure can also be used to construct waveguide micro-ring lasers, as shown in Figure 3-6. The active laser medium is in the ring. The ring resonance results in the desired cavity. The laser output is achieved by tapping a small portion of laser light to the output channel through a directional coupling technique. The use of a micro-ring ensures the wide free spectral range necessary for communications and data processing applications.

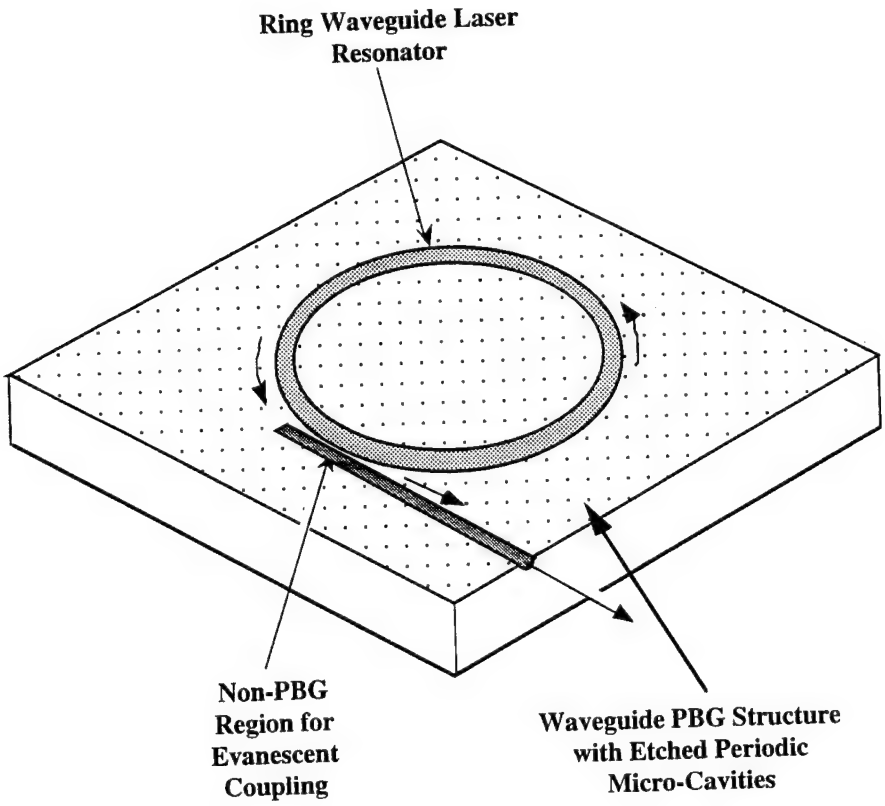

Figure 3-6
Waveguide PBG-based micro-ring laser.

The waveguide PBG structure can also be used to construct compact waveguide delay lines (Figure 3-7) for phased-array antenna and radar applications. Currently, waveguide delay lines of 10 m long, -17 dB total loss, have been achieved on silica-on-silicon with 9 x 6 cm size. Using the proposed small bending radius, the resulting device can be more compact.

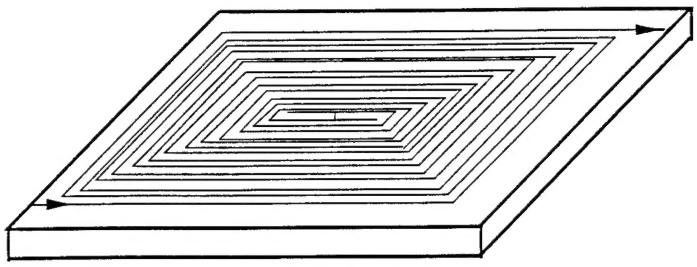

Figure 3-7
Construction of waveguide delay lines for phased array antenna and radar applications.

A waveguide PBG structure based on high reflectivity and wide wavelength and angular bandwidths can be used to construct high reflectivity waveguide mirrors or beam splitters (using finite structure periods) with any small incident angle. This is currently impossible using presently available waveguide devices based on the total internal reflection concept. Figure 3-8 shows a small angle waveguide mirror. The realization of such mirror or beam splitter (partial reflecting and partial transmitting) can facilitate the formation of a variety of integrated optical computing systems by integrating bulk optical computing and signal processing systems into a waveguide. High reliability and compactness of the computing systems can thus be achieved. The waveguide PBG structure can also be used to enhance the reflectivity of waveguide Rowland circle gratings for waveguide wavelength division multiplexers and demultiplexers (WDM) (see Figure 3-9). Without the waveguide PBG structure, the present device has insertion loss of about -15 dB. With the waveguide PBG structure, the device loss can potentially be reduced to -5 dB.

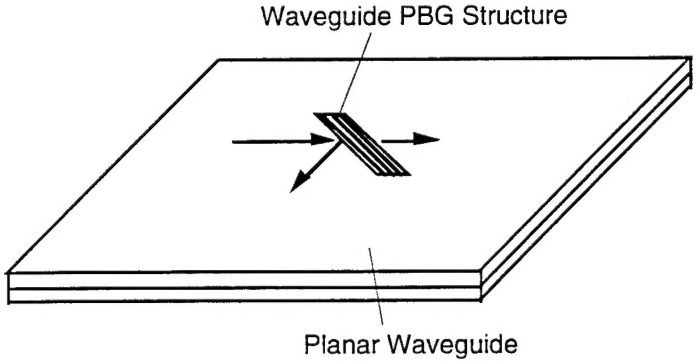

Figure 3-8
Use of waveguide PBG structure for constructing high reflectivity waveguide mirrors for beam splitting and computing systems.

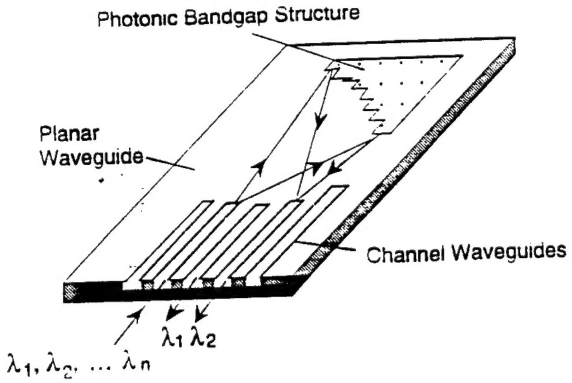

Figure 3-9
Waveguide PBG grating for low loss waveguide WDM devices.

4.0 CONCLUSIONS

Physical Optics Corporation (POC) proposed a new concept of creating photonic band gaps on optical waveguides for the realization of low loss bends. These low loss bends are particularly useful for the realization for optical buses for high density interconnection networks for multichip modules and other single-board high-speed functional circuits. In the Phase I program, we have focused on those structures that can be used to construct waveguide photonic band gap structures, namely 2-D and 1-D PBG structures. When the depth of the PBG structures are deeper than the waveguide mode confinement, the guided modes will view the finite etched depth as an infinite structure, and thus conventional approaches assuming infinite PBGs can be adopted in our formulation. The theory for conventional 1-D and 2-D photonic band gap structures has been well developed. However, none of them has addressed the confinement of propagating light beams between two PBG structures, in either 1-D or 2-D geometries. Confinement of propagating light beams or modes between two 1-D and 2-D PBG structures is the base for the formation of the channel waveguide, and thus for the formation of low loss sharply bent channels. In Phase I, POC examined this issue in greater detail, especially for the case using 1-D PBG structures for the confinement of propagating light. The 2-D PBG structure is found to be highly polarization dependent, and requires large differences in refractive indices to establish band gaps. The 1-D PBG requires less index difference, and in some cases is polarization-independent. This makes it very attractive for the construction of channel waveguides of our interest.

The detailed properties of the confinement of light beams between two 1-D PBG structures are summarized as follows. At small off-axis beam angle, the light confinement between the two 1-D PBG structure is excellent which is similar to conventional waveguide. At off-axis angle of 33°, the beam confinement is still good with most energy confined in the center region and not side lobes in the PBG regions. This is not achievable in conventional singlemode optical waveguide. Further increasing the off-axis angle results in some energy penetration into the PBG regions with observable side lobes. The light beam confinement is still good even under 90° off-axis angle. No energy is lost due to leakage. The effect of the width of the center region is not obvious in our calculation examples showing not fundamental changes in beam confinement features. It is expected that increasing the width will eventually result in a multimode confinement.

Experimental realization of the PBG structure on polymer has not been performed in Phase I, due to the high cost of the non-recurring engineering fee. The estimated cost is about $15,000. This high cost demonstration is unrealistic in Phase I, and thus the experimental demonstration has been postponed to Phase II. We know that the realization of the PBG structure on polymer is practically achievable based on the following factors: a) The polymer index is large enough; and b) The period of the structure is large enough to allow practical realization of the structure by reactive ion beam etching techniques. Thus, the experimental realization of the proposed PBG structure for low loss channel waveguide is feasible and is expected. The potential cost for each structure can be very low (under $50/piece) with large fabrication volumes based on mature semiconductor processing techniques. This facilitates practical applications in a variety of commercial markets.

The potential applications of the waveguide PBG structure have been summarized in Section 3.0. These applications include low loss sharply bent channel waveguide optical buses, waveguide notch filters for communication and sensing applications, construction of micro-ring wavelength filters, micro-ring multiwavelength crossbar switches, micro-ring based WDM devices, micro-ring lasers, low loss waveguide delay lines for optically controlled phased-array antenna systems, construction of waveguide mirrors and beam splitters for integrated optical computing and signal processing systems, and low loss Rowland circle grating-based waveguide WDM devices. Since the waveguide PBG structure is a generic component, its impact on new structures, device components, and systems will be significant. It can be considered as an enabling technology for a variety of research fields.

5.0 REFERENCES

1. E. Yablonovitch, "Photonic Band-Gap Structures," J. Opt. Soc. Am. B, **10**(2), 283-295 (1993).
2. P. S. J. Russell, "Photonic Band Gaps," Physics World, August, pp. 37-42 (1992).
3. S. John, "Localization of Light," Physics Today, **44**, 32 (1991).
4. J. P. Dowling and C. M. Bowden, "Best Radiation from Dipoles Near A Photonic Band edge," J. Opt. Soc. Am. B, **10**(2), 353-355 (1993).
5. N. F. Johnson and P. M. Hui, "K.P Theory of Photonic Band Structures in Periodic Dielectrics," J. Physics: Condensed Matter, **5**(29), L355-L360 (1993).
6. A. A. Maradudin and A. R. McGurn, "Photonic Band Structure of a Truncated, Two-Dimensional, Periodic Dielectric Medium," J. Opt. Soc. Am. B, **10**(2), 307-313 (1993).
7. D. R. Smith, R. Dalichaouch, N. Kroll, S. Schultz, et al., "Photonic Band Structure and Defects in One and Two Dimensions," J. Opt. Soc. Am. B, **10**(2), 314-321 (1993).
8. R. D. Meade, A. M. Rappe, K. D. Brommer, and J. D. Joannopoulos, "Nature of the Photonic Band Gap: Some Insights from A Field Analysis," J. Opt. Soc, Am. B, **10**(2), 328-332 (1993).
9. S. Datta, C. T. Chan, K. M. Ho, and C. M. Soukoulis, "Photonic Band Gaps in Periodic Structures: The Scalar-Wave Approximation," Physical Review B, **46**(17), 10650-10656 (1992).
10. E. Yablonovitch, T. J. Gmitter, R. D. Meade, A. M. Rappe, et al., "Donor and Acceptor Modes in Photonic Band Structure," Physical Review Letters, **67**(24), 3380-3383 (1991).
11. M. Phihal and A. A. Maradudin, "Photonic Band Structure of Two-dimensional Systems: The Triangular Lattice," Physical Review B, **44**(16), 8565-8571 (1991).

12. S. Satpathy and Ze Zhang, "Electromagnetic Wave Propagation in Periodic Dielectric Media: The Photonic Band Structure," Modern Physics Letters B, **5**(16), 1041-1054 (1991).
13. S. John and J. Wang, "Quantum Optics of Localized Light in a Photonic Band Gap," Physical Review B, **43**(16), 12772-12789 (1991).
14. M. Phihal, A. Shambrook, A. A. Maradudin, and Ping Sheng, "Two-Dimensional Photonic Band Structures," Optics Communications, **80**(3-4), 199-204 (1991).
15. E. Yablonovitch, T. J. Gmitter, K. M. Leung, R. D. Meade, et al., "3-Dimensional Photonic Band Structure," Optical and Quantum Electronics, **24**(2), S273-S283 (1992).
16. E. Özbay, E. Michel, G. Tuttle, R. Biswas, M. Sigalas, and K. M. Ho, "Micromachined Millimeter-Wave Photonic Band-Gap Crystals," Appl. Phys. Lett., **64**(16), pp. 2059-2061 (1994).
17. T. Miyashita, S. Sumida, and S. Sakaguchi, "Integrated Optical Devices Based on Silica Waveguide Technologies," Proc. SPIE, Vol.993, 288-294 (1988).
18. E. A. J. Marcatili, "Bends in Optical Dielectric Guides," Bell Syst. Tech. J. p.2103-2132 (1969).
19. K. Thyagarajan, M. R. Shenoy, and A. K. Ghatak, "Accurate Numerical Method for the Calculation of Bending Loss in Optical Waveguides Using A Matric Approach," Opt. Lett., **12**(4), 296-298 (1987).
20. M. Miyagi, "Bending Losses in Hollow and Dielectric Tube Leaky Waveguides," Appl. Opt., **20**(7), 1221-1229 (1981).